Plant, Cell & Environment

Plant, Cell and Environment (2015) **38**, 2088–2097 doi: 10.1111/pce.12532

Original Article

Force–displacement measurements of earlywood bordered pits using a mesomechanical tester

Samuel L. Zelinka[1], Keith J. Bourne[1], John C. Hermanson[2], Samuel V. Glass[1], Adriana Costa[3] & Alex C. Wiedenhoeft[3]

[1]Building and Fire Sciences, [2]Engineering Mechanics and Remote Sensing Laboratory and [3]Center for Wood Anatomy Research, Forest Products Laboratory, U.S. Forest Service, Madison, WI 53726, USA

ABSTRACT

The elastic properties of pit membranes are reported to have important implications in understanding air-seeding phenomena in gymnosperms, and pit aspiration plays a large role in wood technological applications such as wood drying and preservative treatment. Here we present force–displacement measurements for pit membranes of circular bordered pits, collected on a mesomechanical testing system. The system consists of a quartz microprobe attached to a microforce sensor that is positioned and advanced with a micromanipulator mounted on an inverted microscope. Membrane displacement is measured from digital image analysis. Unaspirated pits from earlywood of never-dried wood of *Larix* and *Pinus* and aspirated pits from earlywood of dried wood of *Larix* were tested to generate force–displacement curves up to the point of membrane failure. Two failure modes were observed: rupture or tearing of the pit membrane by the microprobe tip, and the stretching of the pit membrane until the torus was forced out of the pit chamber through the pit aperture without rupture, a condition we refer to as torus prolapse.

Key-words: air seeding; mesomechanical testing; pit membrane; torus prolapse; wood preservative treatment.

INTRODUCTION

At the mesoscale (1–1000 μm), subcellular structures of softwood tracheids (e.g. cell wall thickenings, warty layer, pitting to adjacent cells) are the dominant observable features, and measuring the mechanical properties of these features can give insight into plant physiological aspects of living trees and commercially important lumber processes, such as kiln drying and preservative treatment. The single most prominent subcellular feature of tracheids is the presence of circular bordered pits. Circular bordered pits are structurally complex thin areas in the cell walls through which sap flows from cell to cell in the living tree, and which are reported to play critical roles in preventing the spread of embolism (Sperry & Tyree 1988). The bordered pit is delimited by borders, arching curves of cell wall in which the pit apertures are found, Fig. 1a. Once a fluid passes through the pit aperture it enters the pit chamber, and there encounters the pit membrane. The pit membrane has two domains, the cellulosic reticulum of the margo (Fig. 1a) through which fluids can flow by traversing capillaries within the reticulum, and a central, thickened torus of pectic material overlying and penetrating the cellulosic reticulum beneath, with a diameter greater than that of the pit apertures. To pass from cell to cell, fluids must flow through the margo and then into the adjacent pit chamber, then out through the pit aperture into the adjacent cell lumen. In the presence of pressure differentials of as-yet-unknown magnitude (caused by air bubbles or full embolism), the bordered pit reportedly (Gregory & Petty 1973; Sperry & Tyree 1990; Pittermann *et al*. 2005; Cochard 2006; Cochard *et al*. 2009) acts like a valve; the margo stretches as pressure appresses the torus against the inner face of the border, creating a transient seal that prevents the air bubble from expanding into the adjacent cell. This state of the torus seating against the inner face of the border and sealing the pit aperture is called aspiration, and in the living tree is reversible and presumably extremely common. When the tree is felled and begins to dry, the earlywood pits aspirate (Bao *et al*. 2001). Pit aspiration is also a common part of heartwood formation in many taxa, and the deposition of extractives in the lumina and across the pit membranes of tracheids with aspirated pits (Sano 1998) permanently reduces the permeability of the wood (Fujii *et al*. 1997). The process of aspiration in both living and dead trees (lumber) is of great importance, and at least in living trees, is the subject of much current research.

Much of the current effort on understanding bordered pits in living trees is focused on air seeding, the process by which a pit membrane fails and allows air to 'seed' to the adjacent cell (Gregory & Petty 1973; Sperry & Tyree 1988, 1990; Hacke *et al*. 2004; Pittermann *et al*. 2005; Usta 2005; Cochard 2006; Choat *et al*. 2008; Cochard *et al*. 2009; Delzon *et al*. 2010; Jansen *et al*. 2012). Several different mechanisms have been proposed for this process: capillary seeding, where air travels through capillaries in the margo; stretch seeding, where the torus is pushed out of the aperture; seal seeding, where the torus is not fully appressed to the inside of the border; and rupture seeding, where some part of the pit membrane breaks (Delzon *et al*. 2010). We illustrate these mechanisms in Fig. 1, adapted from the illustration of Delzon *et al*. (2010). Based on measurements of hydraulic conductivity, pit

Correspondence: S. L. Zelinka. e-mail: szelinka@fs.fed.us

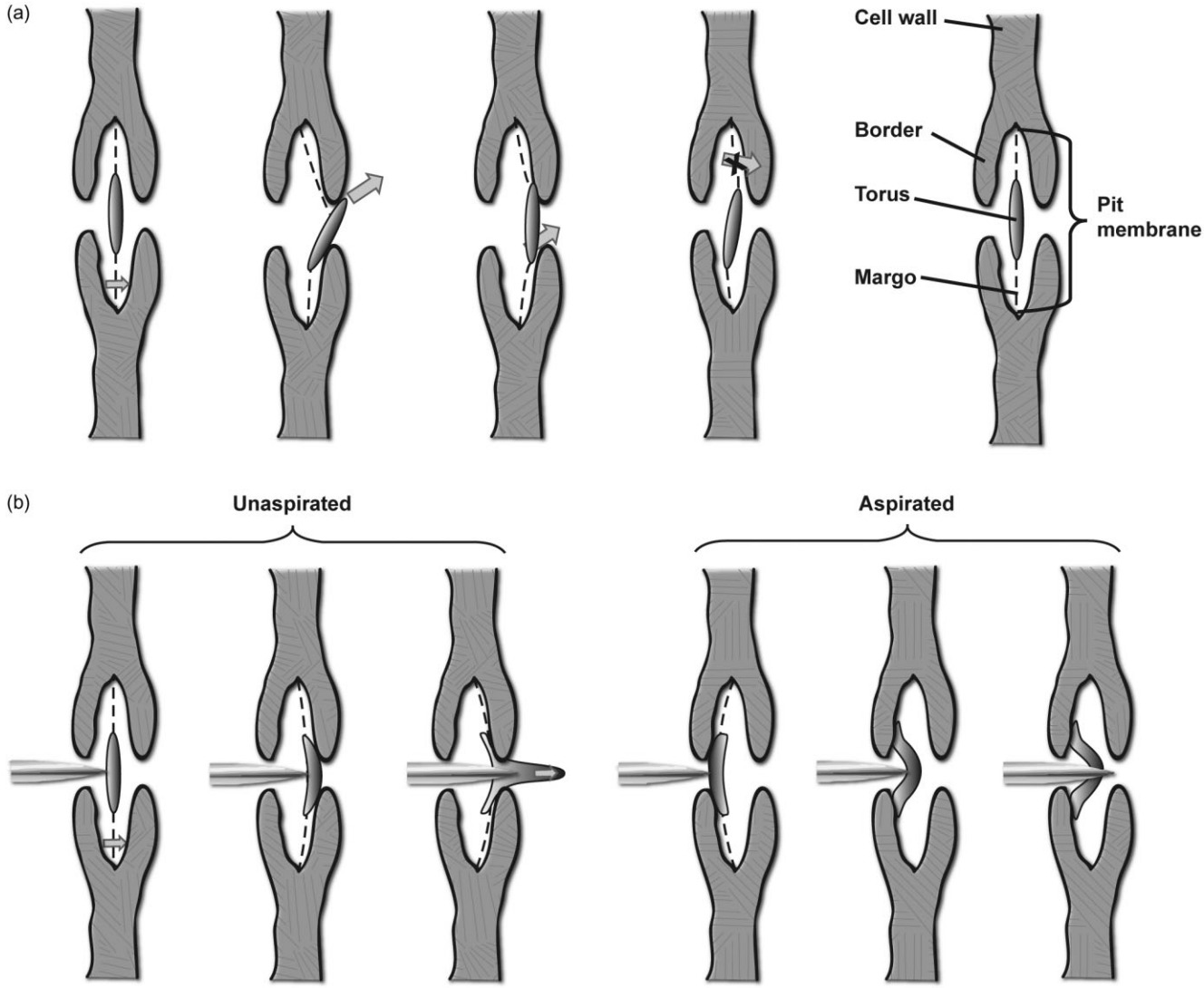

Figure 1. Top (a) mechanisms of air seeding proposed by Delzon with a labelled schematic of a bordered pit on the far right (Delzon *et al.* 2010). From left to right, margo capillary seeding, margo stretch seeding, seal capillary seeding, margo rupture seeding. Bottom (b) schematic illustration of the deformation of the pit membranes of unaspirated and aspirated pits.

geometry and assumed elastic properties of the pit membrane, arguments for and against each of these types of air-seeding mechanisms have been made (Sperry & Tyree 1990; Hacke *et al.* 2004; Delzon *et al.* 2010; Jansen *et al.* 2012). To date, there have been no direct observations of any of these mechanisms. Two consistent themes in these analyses are that the torus is (implicitly) treated as a rigid object and accurate measurement of elastic properties of the pit membrane are necessary to go beyond the speculation of the mechanism(s) of air seeding.

The aspiration of bordered pits is also important for wood technology, specifically in wood drying and wood preservation (Petty & Puritch 1970; Flynn 1995; Singh *et al.* 1999; Bao *et al.* 2001; Usta & Hale 2006; Wang & Sugiyama 2011). Kiln drying schedules have been developed to remove moisture from wood under controlled conditions to prevent uneven drying and minimize the attendant drying defects (Boone *et al.* 1988). This process is complicated by the fact that the cells closest to the edge of the wood dry first, causing pit aspiration. Pit aspiration removes direct cell-to-cell pathways for bulk water vapour movement thus lowering the vapour permeability of the wood and slowing further drying. Preservative treatments are applied to wood by submersing lumber in a preservative treatment solution and applying cycles of vacuum and pressure. Preservative penetration by this method varies by wood species, and aspirated pits are rate-limiting factors in preservative treatment (Lebow 2010). Several researchers have shown that destroying the pit membranes using enzymes or fungi increases uptake of treatment chemicals at the meter scale, and increases the longitudinal gas permeability of the wood (Tschernitz 1973; Schwarze *et al.* 2006; Schwarze 2008; Lehringer *et al.* 2009) at the centimetre scale.

MATERIALS AND METHODS

Here, we introduce a method for taking the force–displacement measurements of unaspirated and aspirated bordered pits and demonstrate its capability by presenting data measured across two genera.

While there are many mechanical test systems operating at the macroscale and at the nanoscale, the mesoscale is comparatively neglected. In order to conduct mechanical tests on circular bordered pits, a mesoscale tester from commercial off-the-shelf components was assembled (Fig. 2). Force was measured through a microforce sensor and displacement was analysed by image analysis from videos recorded during the experiments.

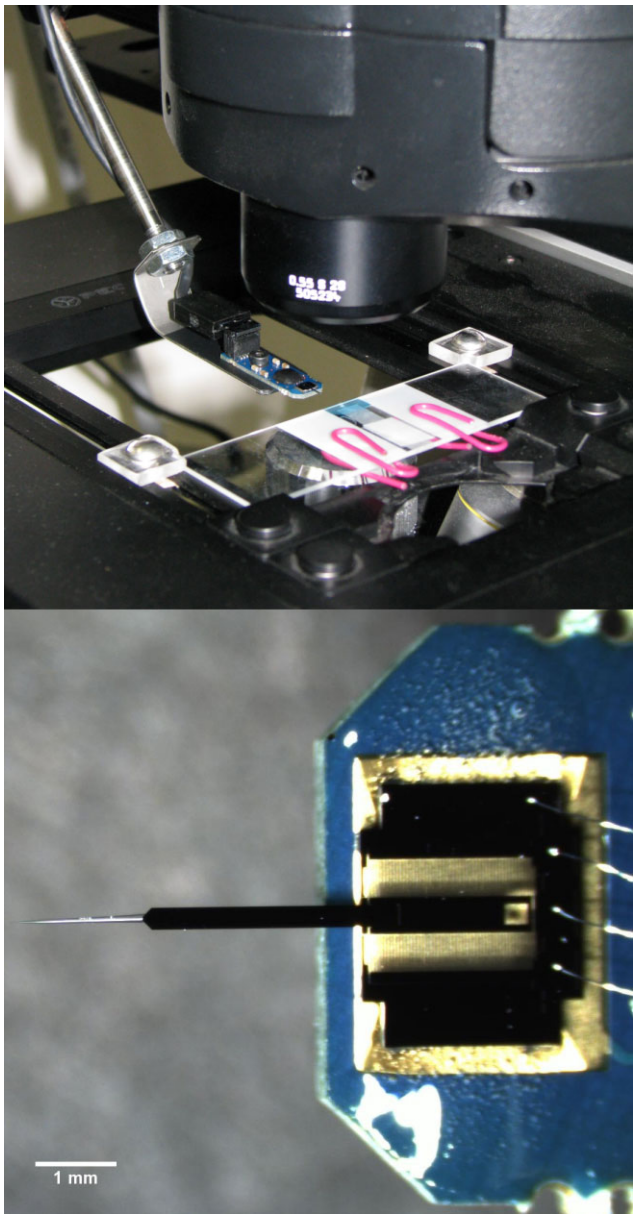

Figure 2. Top – mesomechanical tester showing the specimen grips, microforce sensor microscope stage. The microforce sensor was controlled with a micromanipulator and used to manipulate tissue observed in the inverted microscope. Bottom – close-up view of the microforce sensor illustrating the attached quartz probe.

The mesomechanical testing system consisted of an inverted microscope (Leica DMI 6000 Wetzlar, Germany) with a motorized mechanical stage (Leica STP 6000 Wetzlar, Germany controlling a Marzhauser EK 127×83 Wetzlar, Germany), a computer-controlled three-axis micromanipulator (MP-285, Sutter Instruments, Novato, CA, USA), and a capacitive microforce sensor (model FTS-1000, Femto Tools, Buchs, Switzerland) modified with a solid quartz micropipette used as a probe. The microscope was fitted with a Grasshopper Express 2.8 MP camera (Point Grey Research, Richmond, BC, Canada). The wood specimen was mounted on a glass slide and positioned with the mechanical stage; the microforce sensor and probe are controlled with the micromanipulator. Force was measured through the microforce sensor and displacement was analysed by image analysis from videos recorded during the experiments.

Probe tips were pulled from a solid quartz capillary (1 mm in diameter) with a programmable laser micropipette puller (Sutter Instruments, P2000) using a custom routine (parameters: heat: 900; filament: 4; velocity: 55; delay: 130; pull: 60), which would repeat three times on a successful pull. The outer geometry of the pipette tip was between that of a patch-clamp electrode and a microelectrode (Fig. 2). The diameter at the point was 0.7 μm, and the area immediately adjacent to the tip (generated from the third loop through the programme) had an angle of 16°. It should be noted that the total angle from the 10 mm to the tip was much less than the 16° from the third pull, which is why, at low magnification, the tip looks much sharper than it actually is. The pipette tip was broken from the pipette with a diamond scribe and was glued to the end of the microforce sensor.

The microforce sensor was used to measure the applied force. The microforce sensor had a sensitivity of 500 μN V^{-1} and a maximum force of 1000 μN, with a quoted resolution of less than 0.05 μN. Microforce sensors were factory calibrated against SI standards and the gain from the individual calibrations was supplied with the sensors. The force–displacement measurements were made by manually incrementing the micromanipulator to which the microforce sensor was attached. The step size was set to 62.5 nm per step.

Tangential sections 35 μm thick were cut using a sliding microtome and stored in 25% ethanol prior to manipulation to prevent fungal growth. After removal from storage, sections were stained with 1% aqueous Alcian Blue to increase the contrast of the tori to improve automatic tracking with image analysis routines. No difference in force measurements could be detected between tests on stained and unstained pit membranes. The experiments were conducted in aqueous conditions (Fig. 3). Sections were placed on a glass microscope slide so that they were approximately 0.5 mm behind the edge of the slide. Adhesive tape was placed over the slide under the sides of the sample and acted as a spacer. A coverslip was placed over the tape and held in place by two torsional springs. A piece of tissue paper was in contact with the section and protruding from under the coverslip so that

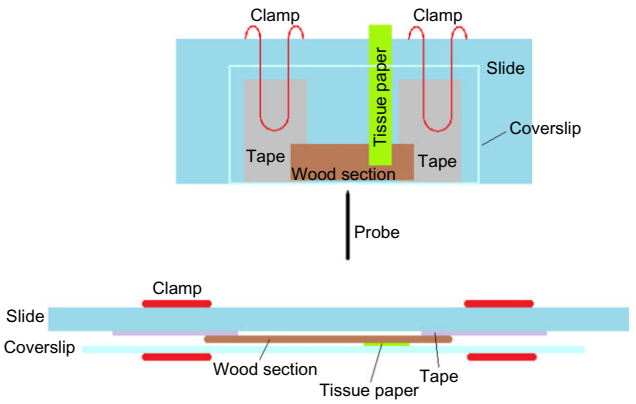

Figure 3. Schematic diagram of the experimental set-up and the probe tip.

water could be added to the specimen after it had been placed in the microscope.

Because the focal plane of the tip in air was different from the focal plane of the pit membrane, care was needed to introduce the tip to the aqueous media between the slide and the upper coverslip in the 0.5–1.0 mm gap between the edge of the slide and the edge of the wood section. The focal depth of the top of the coverslip and the bottom of the slide were measured, and then the probe was brought into the same focal plane as the bottom of the slide. The probe height was then lowered to one-half of the total distance between the slide and the coverslip and the focal depth was adjusted so that the wood section was in focus, and then the probe was advanced blindly, until it penetrated the water meniscus at which point it was brought to the same focal depth of the wood section.

Displacement was measured from the videos with a computer programme written using cross-correlation subroutines supplied with Matlab R2013b (Mathworks Software, Natick, MD, USA). The recorded videos are first converted to 8 bit greyscale format. To track an object such as the probe or a portion of the cell, a region of interest (ROI) is selected around the object. Then, for each frame in the movie a normalized two-dimensional cross-correlation calculation is performed using Matlab's *normxcorr2* function. The *normxcorr2* function is called with the first input being the ROI previously selected and the second input being the current frame of the video. For each frame, the cross-correlation function outputs a correlation coefficient matrix. The maximum value in the correlation coefficient matrix indicates the location where the ROI best lines up with the picture in the frame. By keeping track of the location of the maximum correlation coefficient in each frame of the video, the relative location of the ROI and the object within it can be tracked throughout the video.

The tip position was determined by selecting a ROI on the pipette far away from the bordered pit and using the autocorrelation routines described earlier to track this ROI. Tip position measured this way matched the change in position commands sent to the micromanipulator, and displacement measured with either of these techniques corresponded to the displacement of the pit membrane. To illustrate that these displacements correlated with the displacement of the pit membrane, Tracker plugin with ImageJ 1.48t (National Institutes of Health, Bethesda, MD, USA) was used to track the centroid of a pit membrane and compare it with the displacement output from the micromanipulator and the displacement from the autocorrelation routines. The results of are presented in Fig. 4. Starting with an RGB format colour video of a force–displacement measurement on a sample with membranes that were stained with Alcian blue, the ImageJ *Colour Threshold* function was used to adjust the threshold values of the hue, saturation and then the brightness of the video to convert the video to binary with just the pit membrane remaining. Then the ImageJ Tracker plugin was used to track pit membrane position throughout the video. The Tracker plugin outputs a text file with the coordinates of the centroid of the object in each frame. When the tip is in contact with the pit membrane, all three are in agreement until the pit membrane is in contact with the back border of the cell wall, at which time the pit membrane deforms out of plane, thus changing the centre of mass as recorded in the microscope image. Figure 4 illustrates that either the autocorrelation routines or the micromanipulator position could be used to determine the location of contact between the tip and the pit membrane.

In some cases, the entire cell wall-bordered pit structure was translated. The amount of cell wall translation was measured by also tracking the cell wall with the *normxcorr2* function in Matlab. Because the cell wall also moved during the

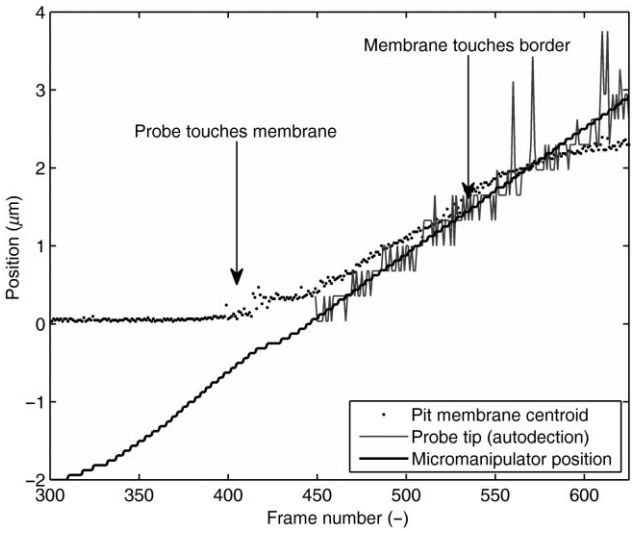

Figure 4. Comparison of the three methods for determining position – tracking the centroid of the pit membrane through image detection (dots), tracking the probe tip through image detection (thin line) and measuring the readout of the micromanipulator position (thick line). The probe tip contacted the pit membrane in approximately the 500th frame. In the 580th frame of the video, the pit membrane came in contact with the border and experienced out of plane deformation, which caused the centroid to change and not move with the probe tip.

measurements, the slopes of the force versus displacement curves cannot be directly related to the stiffness of the pit membrane.

Unaspirated earlywood pits were measured in two species: *Pinus strobus* and *Larix laricinia*. Both specimens were collected in southern Wisconsin (approximately 43° N latitude) and removed from the bole of the tree. Experiments were also performed on aspirated earlywood pits in a xylarium specimen, (MADw 15542) of *L. laricinia*.

RESULTS

Image series from a subset of the videos (included as Supporting Information) are shown to illustrate the experiments and failure mechanisms. Examples of the force versus displacement curves are presented for aspirated and unaspirated *Larix larcinia* (hereafter referred to as *Larix*) and summary data (i.e. maximum force, deflection, tip size, failure mode) are presented for *Pinus strobus* (hereafter referred to as *Pinus*).

We show a sequence of video screen captures ($\Delta t = 7.46$ s) of torus displacement and deformation in a typical unaspirated pit in *Larix* (Fig. 5). Additional replicates exhibited similar deformation characteristics and one of two failure modes. In most cases, the pit membrane failed when the probe tip ruptured (tore) the pit membrane, but in some cases, the torus prolapsed, forced out of the pit chamber through the pit aperture without rupture.

The corresponding force–displacement curve associated with the image sequence of the unaspirated pit shown in Fig. 5 is shown in Fig. 6. The zero of the displacement is defined as the front of pit membrane as seen by the probe (the upper left side in Fig. 5). The amount of cell wall translation is included for reference. The pit membrane is approximately 2 μm thick.

In the first 2 μm of travel, the pit membrane is being displaced within the chamber and the force required is less than the noise level in our measurements (about 3 μN). The force required to move the torus to the aspirated condition is less than or equal to the noise floor of the measurements (3 μN). The displacements within the pit chamber are fully elastic; in several experiments, the probe was removed and the pit membrane returned to its measured starting position.

Figure 7 shows images taken from a video where an aspirated pit (in *L. laricinia*) was pushed until the pit ruptured ($\Delta t = 2.87$ s); the movie is included as Supporting Information. In contrast to the unaspirated pits, the measured force increased as soon as the probe made contact with the pit membrane. In all measurements, the torus ruptured rather than detached from the pit border.

Figure 8 shows the force deflection curve corresponding with Fig. 7; the amount of cell wall translation is also included. In this curve, the zero in displacement (x axis) corresponds with the position of the tip when it first contacts the torus in the aspirated position. Both the forces and displacements were lower than for the unaspirated pits.

DISCUSSION

The purpose of this work was to quantify force–displacement measurements of pit membranes in gymnosperms. This work presents preliminary data showing for the first time, direct measurements of the forces necessary to displace or rupture pit membranes in unaspirated and aspirated pits in the earlywood of two species. The commercial off-the-shelf components were chosen based upon expected air-seeding forces (1–10 mN) from the plant physiological literature on air-seeding hypotheses.

Our mesomechanical testing system is a first attempt with numerous limitations: the noise floor of the microforce sensor was too high to measure the force needed to displace the pit membrane in unaspirated pits; the system only allowed the experiment to be observed in two dimensions; the cell wall was not sufficiently constrained; the probe was only able to move in one dimension during the measurement; and the force could only be detected in the same axis. Despite these limitations, the system gave promising preliminary data: pit membranes were manipulated with the probe tip; force–displacement data were recorded; and videos of the deformation and rupture of the bordered pits were collected.

For the pits starting in the unaspirated condition, little force was required (<3 μN) to displace the torus to the aspirated position. From hydraulic conductivity measurements, researchers have calculated an aspiration pressure difference of between 33 and 470 kPa (Gregory & Petty 1973; Sperry & Tyree 1990; Domec *et al*. 2006). Assuming the pressure measured in these experiments is acting over the area of the pit membrane, the calculated force to aspiration is between 8 and 46 μN, slightly higher than the forces measured with the tester.

For the unaspirated pits, not only was the force to move the pit membrane in the chamber below the noise floor, but the force remained unmeasurable until the probe tip reached a position in line with the far borders the pit chamber (Fig. 6), that is, the probe tip had to move through the equivalent thickness of the torus before recording measurable force, demonstrating that the torus is extremely compliant, and that it exhibits significant deformations at forces smaller than the noise floor (3 μN). This is consistent with our observations of torus prolapse and the severe torus deformations we observed at failure. For both aspirated and unaspirated pits, when the pit membrane was constrained by the pit border, the centre of the torus could be pushed approximately 4 μm further before tearing, an additional displacement of roughly twice the thickness of the torus. While previous illustrations of the aspiration mechanism treated the torus as perfectly rigid, we found that the torus was extremely compliant, and in some cases could be deformed so much that it slipped through the pit border. These measurements are a unique demonstration of extreme compliance of the torus and the pit membrane, although torus prolapse is unlikely *in planta* because the pressure would be applied evenly across the entire bearing surface of the border rather than just over the area of the pit aperture.

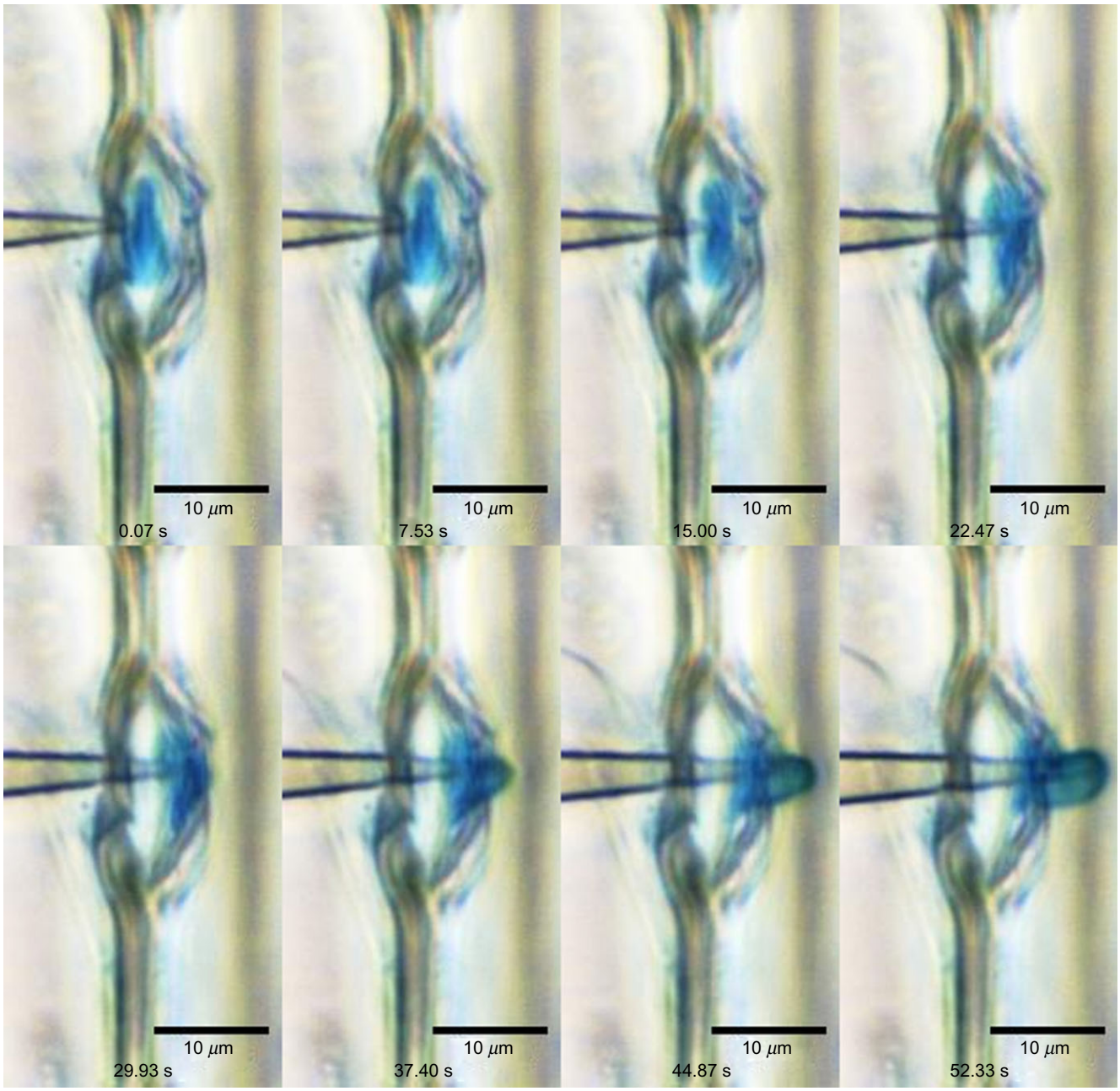

Figure 5. Image series taken from a video of an experiment on an unaspirated bordered pit in *Larix laricinia*. The pit membrane failed when the probe tip penetrated the pit membrane.

In *Larix*, the average maximum force at failure was calculated to be 60 μN (Table 1) and significant deformations (i.e. the 34.7 s frame of Fig. 5) occurred at forces as low as 10 μN. These forces cannot easily be reduced to a stress, as the force was concentrated around the tip in a complex stress state. Domec *et al*. (2006) measured air-seeding pressures in Douglas fir (*Pseudotsuga menziesii*) using the air injection method of Cochard *et al*. (1992) and reported air-seeding pressures of between 3.8 and 9.6 MPa, and also report the diameter of the pit apertures (3.5–6.9 μm). In these experiments, the pressure difference acts across the area of the pit aperture, allowing an estimate of an evenly distributed force needed to cause air seeding in these measurements of between 72 and 190 μN. Although the point force applied in this measurement cannot be directly compared with an evenly distributed pressure difference, it is worth noting that the range of measured forces that may cause air seeding (10–60 μN) are of the same order of magnitude as previous air-seeding measurements.

The reversibility of aspiration (embolism repair) in living plants is important for plant physiological processes and is the topic of recent research (Holbrook & Zwieniecki 1999;

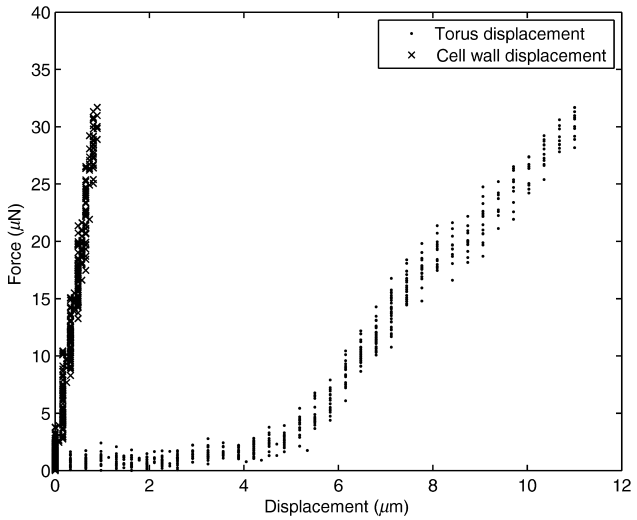

Figure 6. Example force–displacement curves for an unaspirated bordered pit in *Larix laricinia*. The 'torus displacement' curve is the total distance the torus moved relative to its starting position. The cell wall displacement represents the amount of translation the cell wall exhibited. The net displacement of the torus within the pit chamber can be found by subtracting the cell wall displacement from the torus displacement. The cell wall started to translate when the torus force and displacement were 3 μN and 4.9 μm, respectively.

Rockwell *et al*. 2014). The aspirated torus did not detach from the pit border, as would be expected in an embolism repair, but instead ruptured. However, the aspirated pits tested in these experiments came from xylarium samples that had sat in a dry condition for many years. It is possible that during the wood drying process and ensuing storage under dry conditions, irreversible changes occurred to the pit membrane and/or border that caused the observed behaviour. In short, the fact that tori ruptured in these experiments on dried wood does not necessarily mean that a similar behaviour would be observed *in planta*, and in fact our data show clear reversibility from the aspirated to the neutral position in aqueous conditions when the pit membrane is moved with our system.

The large forces needed either to tear or to prolapse the pit membrane have important implications for wood technological processes involving pressure treatment and kiln drying. Researchers have hypothesized that the pressures involved in the preservative treatment process may damage and thus open some aspirated pits, especially if an oscillating pressure is used (Flynn 1995). However, the pressures used in the treatment process are on the order of 1 MPa, (Singh *et al*. 1999) and are unlikely to cause damage to the pit membrane. It is more likely that the combination of oscillating pressure and the chemical interactions between the preservative solution and the pit membrane–border interface facilitate the de-aspiration rather than the tearing of the pit membranes.

CONCLUSIONS

- The force or calculated pressure needed to displace the pit membrane to an aspirated position was found to be less than 3 μN and is slightly lower than previous calculations of the pressure differences needed to cause aspiration.
- The torus is not completely rigid as had been tacitly assumed in air-seeding models. In some cases, the torus prolapsed through the pit aperture. The fact that the torus is not rigid and can undergo large deformations may have implications for understanding hydraulic architecture of gymnosperms, especially air-seeding models.
- The average force needed to cause torus tearing was found to be 60 μN for the unaspirated *Larix* samples, and appreciable deformations of the torus occurred at forces as low as 10 μN. These forces are of the same order of magnitude as air-seeding forces calculated from previously published hydraulic conductivity measurements.

Directly measuring botanical structures implicated in plant physiological processes can only improve our understanding of those processes and allow us to ask new questions about woody plant physiology. We are currently reconfiguring the system to detect smaller forces to better characterize pit membranes in general, and to explore the relation between climatic data and pit properties on a ring-by-ring basis in earlywood and latewood pits in deciduous and evergreen gymnosperms.

In a broader sense, our mesomechanical testing system will measure other mechanical properties of wood at the mesoscale rather than relying on the hypothesized reasoning

Table 1. Summarized results of the mesomechanical testing showing averages of the maximum force, maximum deformation, and pit membrane size determined from the video

		Number of replicates	Max force (μN)	Max. displacement[a] (μm)	Torus diameter (μm)	Membrane diameter (μm)
Aspirated	*Larix laricinia*	7	14	3	9.7	17.4
Unaspirated	*Larix laricinia*	4	60	10	9.3	14.8
	Pinus strobus	5	60	11	8.4	14.0

[a]The maximum displacement was calculated as the amount the torus moved from its starting position relative to the cell wall. Pits were manipulated with a 0.7 μm diameter probe.

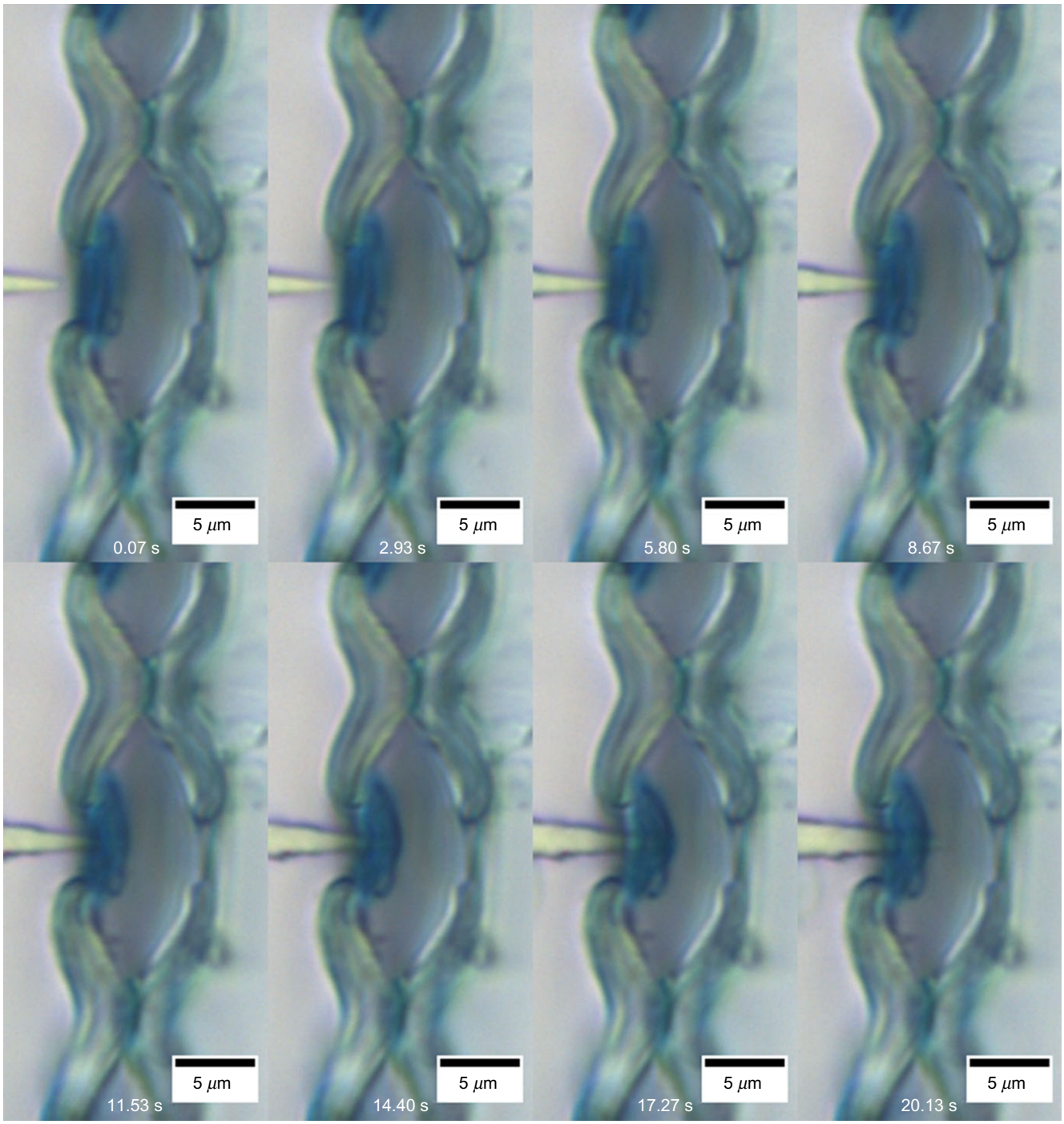

Figure 7. Image series taken from a video of an experiment on an aspirated bordered pit in *Larix laricinia*. The pit membrane failed when the probe tip penetrated the pit membrane.

in the literature. There have been only a few studies examining this spatial scale, and all of them looked at the properties parallel to the long axis of the tracheid (Burgert *et al*. 2002, 2003, 2005; Keunecke *et al*. 2008). This system could be modified to perform bending, compression or tension experiments at length scales between 1 μm and 1 mm. Further logical extensions to the system include observing the sample from multiple axes, manipulating wood cells in multiple axes simultaneously, introducing picolitre volumes of various fluids to observe pit membrane responses, and comparing torus-margo pits to other intertracheary pits in woods that do not exhibit the torus-margo structure.

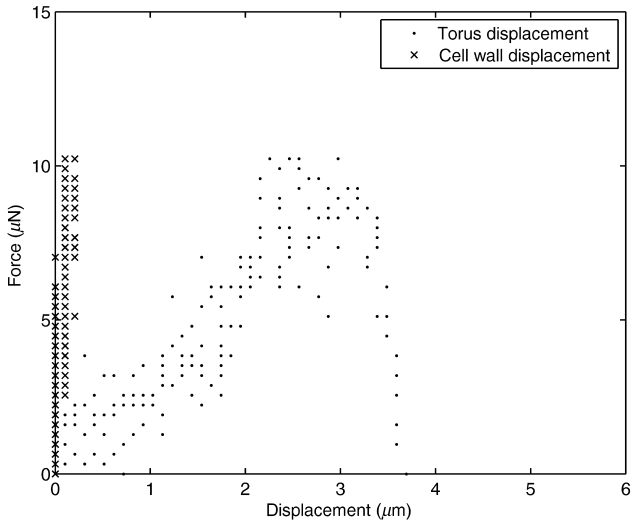

Figure 8. Example force–displacement curves for an aspirated bordered pit in *Larix laricinia*. The 'torus displacement' curve is the total distance the torus moved relative to its starting position. The cell wall displacement represents the amount of translation the cell wall exhibited. The net displacement of the torus within the pit chamber can be found by subtracting the cell wall displacement from the torus displacement.

ACKNOWLEDGMENTS

S.Z. acknowledges funding from a Presidential Early Career Award for Scientists and Engineers (PECASE). The authors acknowledge the assistance of Tivoli Gough of the Forest Products Laboratory for drawing Fig. 1. The contributions from the David Eustice, Richard Jordan and Joseph Destree of the Forest Products Laboratory Machine shop were invaluable in the development of the mesomechanical testing system.

REFERENCES

Bao F., Lu J. & Zhao Y. (2001) Effect of bordered pit torus position on permeability in Chinese yezo spruce. *Wood and Fiber Science* **33,** 193–199.

Boone R.S., Kozlik C.J., Bois P.J. & Wengert E.M. (1988) Dry kiln schedules for commercial woods: temperate and tropical. *General Technical Report, Forest Products Laboratory, USDA Forest Service*.

Burgert I., Keckes J., Frühmann K., Fratzl P. & Tschegg S. (2002) A comparison of two techniques for wood fibre isolation-evaluation by tensile tests on single fibres with different microfibril angle. *Plant Biology* **4,** 9–12.

Burgert I., Frühmann K., Keckes J., Fratzl P. & Stanzl-Tschegg S.E. (2003) Microtensile testing of wood fibers combined with video extensometry for efficient strain detection. *Holzforschung* **57,** 661–664.

Burgert I., Eder M., Frühmann K., Keckes J., Fratzl P. & Stanzl-Tschegg S. (2005) Properties of chemically and mechanically isolated fibres of spruce (*Picea abies* [L.] Karst.). Part 3: mechanical characterisation. *Holzforschung* **59,** 354–357.

Choat B., Cobb A.R. & Jansen S. (2008) Structure and function of bordered pits: new discoveries and impacts on whole-plant hydraulic function. *The New Phytologist* **177,** 608–626.

Cochard H. (2006) Cavitation in trees. *Comptes Rendus. Physique* **7,** 1018–1026.

Cochard H., Cruiziat P. & Tyree M.T. (1992) Use of positive pressures to establish vulnerability curves further support for the air-seeding hypothesis and implications for pressure-volume analysis. *Plant Physiology* **100,** 205–209.

Cochard H., Hölttä T., Herbette S., Delzon S. & Mencuccini M. (2009) New insights into the mechanisms of water-stress-induced cavitation in conifers. *Plant Physiology* **151,** 949–954.

Delzon S., Douthe C., Sala A. & Cochard H. (2010) Mechanism of water-stress induced cavitation in conifers: bordered pit structure and function support the hypothesis of seal capillary-seeding. *Plant, Cell & Environment* **33,** 2101–2111.

Domec J.-C., Lachenbruch B. & Meinzer F.C. (2006) Bordered pit structure and function determine spatial patterns of air-seeding thresholds in xylem of Douglas-fir (*Pseudotsuga menziesii*; Pinaceae) trees. *American Journal of Botany* **93,** 1588–1600.

Flynn K.A. (1995) A review of the permeability, fluid flow, and anatomy of spruce (*Picea* spp.). *Wood and Fiber Science* **27,** 278–284.

Fujii T., Suzuki Y. & Kuroda N. (1997) Bordered pit aspiration in the wood of *Cryptomeria japonica* in relation to air permeability. *IAWA Journal / International Association of Wood Anatomists* **18,** 69–76.

Gregory S. & Petty J. (1973) Valve action of bordered pits in conifers. *Journal of Experimental Botany* **24,** 763–765.

Hacke U.G., Sperry J.S. & Pittermann J. (2004) Analysis of circular bordered pit function II. Gymnosperm tracheids with torus-margo pit membranes. *American Journal of Botany* **91,** 386–400.

Holbrook N.M. & Zwieniecki M.A. (1999) Embolism repair and xylem tension: do we need a miracle? *Plant Physiology* **120,** 7–10.

Jansen S., Lamy J.B., Burlett R., Cochard H., Gasson P. & Delzon S. (2012) Plasmodesmatal pores in the torus of bordered pit membranes affect cavitation resistance of conifer xylem. *Plant, Cell & Environment* **35,** 1109–1120.

Keunecke D., Eder M., Burgert I. & Niemz P. (2008) Micromechanical properties of common yew (*Taxus baccata*) and Norway spruce (*Picea abies*) transition wood fibers subjected to longitudinal tension. *Journal of Wood Science* **54,** 420–422.

Lebow S. (2010) Wood preservation. In *Wood Handbook- Wood as an Engineering Material* (ed. R.J. Ross), p. 508. U.S. Department of Agriculture, Forest Service, Forest Products Laboratory, Madison, WI.

Lehringer C., Richter K., Schwarze F.W.M.R. & Militz H. (2009) A review on promising approaches for liquid permeability improvement in softwoods. *Wood and Fiber Science* **41,** 373–385.

Petty J. & Puritch G. (1970) The effects of drying on the structure and permeability of the wood of *Abies grandis*. *Wood Science and Technology* **4,** 140–154.

Pittermann J., Sperry J.S., Hacke U.G., Wheeler J.K. & Sikkema E.H. (2005) Torus-margo pits help conifers compete with angiosperms. *Science* **310,** 1924.

Rockwell F.E., Wheeler J.K. & Holbrook N.M. (2014) Cavitation and its discontents: opportunities for resolving current controversies. *Plant Physiology* **164,** 1649–1660.

Sano Y. (1998) Time course of the secondary deposition of encrusting materials on bordered pit membranes in *Cryptomeria japonica*. *IAWA Journal* **19,** 285–299.

Schwarze F.W.M.R. (2008) Procedure and composition for the improvement of the uptake and distribution of soaking compositions in woods. European Patent EP1681145.

Schwarze F.W.M.R., Landmesser H., Zgraggen B. & Heeb M. (2006) Permeability changes in heartwood of *Picea abies* and *Abies alba* induced by incubation with *Physisporinus vitreus*. *Holzforschung* **60,** 450–454.

Singh A., Dawson B., Franich R., Cowan F. & Warnes J. (1999) The relationship between pit membrane ultrastructure and chemical impregnability of wood. *Holzforschung* **53,** 341–346.

Sperry J. & Tyree M. (1990) Water-stress-induced xylem embolism in three species of conifers. *Plant, Cell & Environment* **13,** 427–436.

Sperry J.S. & Tyree M.T. (1988) Mechanism of water stress-induced xylem embolism. *Plant Physiology* **88,** 581–587.

Tschernitz J. (1973) Enzyme mixture improves creosote treatment of kiln-dried Rocky mountain Douglas-fir. *Forest Products Journal* **23,** 30–38.

Usta I. (2005) A review of the configuration of bordered pits to stimulate the fluid flow. *Maderas. Ciencia y Tecnología* **7,** 121–132.

Usta I. & Hale M. (2006) Comparison of the bordered pits of two species of spruce (Pinaceae) in a green and kiln-dried condition and their effects on fluid flow in the stem wood in relation to wood preservation. *Forestry* **79,** 467–475.

Wang Y. & Sugiyama J. (2011) Effect of morphological variability of incrusted pit membranes on efficiency of transverse compression to improve liquid uptake. *Holzforschung* **65,** 763–769.

Received 14 November 2014; received in revised form 21 February 2015; accepted for publication 2 March 2015

SUPPORTING INFORMATION

Additional Supporting Information may be found in the online version of this article at the publisher's web-site:

Video Clip S1. Video of an experiment on an unaspirated bordered pit in Larix laricinia. The pit membrane failed when the probe tip penetrated the pit membrane.

Video Clip S2. Video of an experiment on an aspirated bordered pit in Larix laricinia. The pit membrane failed when the probe tip penetrated the pit membrane.